PHYSICAL REVIEW B VOLUME 28, NUMBER 10 15 NOVEMBER 1983

Theory of the nonmetal-metal transition in rare-earth compounds. II. Electrical resistivity and dynamical conductivity

Hideaki Ishikawa*
Department of Physics, Tokyo Metropolitan University, Setagaya-ku, Tokyo 158, Japan
(Received 7 March 1983)

The electrical resistivity and the dynamical conductivity of rare-earth compounds which show the nonmetal-metal transition with increasing temperature are presented. The calculation is based on the physical picture that the hybridization gap vanishes continuously by the spin-field fluctuation with increasing temperature. The electrical resistivity has different temperature dependence below and above the transition temperature. The electrical resistivity at 0 K is infinite. Below the transition temperature, the electrical resistivity lowers abruptly with increasing temperature. The Arrhenius plot of the resistivity versus inverse temperature is not linear. Above the transition temperature, the electrical resistivity decreases rapidly at first and then slowly with increasing temperature. Near 0 K, the dynamical conductivity has an energy absorption edge and a sharp peak at a finite frequency (near twice the hybridization), which is a semiconducting profile. With increasing temperature, the maximum of the conductivity at the finite frequency lowers, and the dynamical conductivity near the zero frequency grows rapidly. At very high temperatures above the transition temperature, the dynamical conductivity has the maximum at the zero frequency and is a decreasing function of frequency, which is a metallic profile.

I. INTRODUCTION

In the preceding paper[1] (hereafter referred to as I) we have described a theory of the nonmetal-metal transition with increasing temperature in rare-earth compounds described by the nondegenerate periodic Anderson model. The essential point of the theory is that the hybridization gap vanishes continuously by virtue of the spin-field fluctuation with increasing temperature. Characteristic parameters of the system are the intra-atomic Coulomb repulsion between f electrons and the hybridization between s and f electrons. In the intermediate region where these two parameters are of the comparative order of magnitudes, the spin-field fluctuation grows in proportion to the square root of temperature at very low temperature compared with the width of the uncorrelated s electron band. The spin-field fluctuation makes the hybridization gap decrease rapidly and vanish at the transition temperature.

In this paper we investigate temperature dependence of the electrical resistivity and the dynamical conductivity based on the above picture. In contrast to previous theories[2-4] on the electrical conductivity, our theory takes into account both the temperature dependence of the density of states and that of the Fermi-Dirac distribution function. In the present theory, the ground state is assumed to be insulating (semiconducting).[2,3] Also an assumption of the mobility gap is unnecessary.[3]

In Sec. II we shall describe the expression of the electric current operator in the periodic Anderson model described in I. We derive the general expression of the electrical conductivity (the Kubo formula[5]) in the functional integral representation. In Sec. III we shall introduce approximations: the static approximation and the single-site coherent-potential approximation (CPA). In Sec. IV we shall introduce simple assumptions on the parameters in the model Hamiltonian. We assume the elliptic model density of states for the uncorrelated s electron band. In Sec. V we show the results of the numerical calculation using the same parameters described in I. Finally we discuss the qualitative comparison of our results with experiments.

II. GENERAL FORMULA OF THE ELECTRICAL CONDUCTIVITY

A. The electric current in the model Hamiltonian

A model Hamiltonian of rare-earth compounds is the periodic Anderson model[1,6] which is an array of "Anderson impurities."[7] The detailed form of the Hamiltonian $\hat{H}$ is given by Eqs. (2.1)—(2.9) in I. The total electric current operator $\hat{J}_\mu$ is the product of charge e and a velocity operator of electron $\hat{v}_\mu$,

$$\hat{J}_\mu = e\hat{v}_\mu \ . \tag{2.1}$$

The velocity operator is the derivative of a position operator of electron $\hat{\vec{r}}$ with respect to time t. The position operator in the second quantized representation is given by

$$\hat{\vec{r}} = \sum_{m,\sigma} \vec{R}_{m\sigma}(c^\dagger_{m\sigma}c_{m\sigma} + f^\dagger_{m\sigma}f_{m\sigma}) \ , \tag{2.2}$$

where $\vec{R}_{m\sigma}$ is the lattice vector, $c_{m\sigma}$ and $f_{m\sigma}$ are the annihilation operators of s and f electrons. We obtain the general expression of the velocity operator from the Heisenberg equation of motion:

$$\hat{v}_\mu=\frac{d\hat{r}_\mu}{dt}=\frac{1}{i}[\hat{r}_\mu,\hat{H}]$$
$$=\sum_{\vec{k},\sigma}\frac{\partial\epsilon_{c\vec{k}\sigma}}{\partial k_\mu}c^\dagger_{\vec{k}\sigma}c_{\vec{k}\sigma}+\sum_{\vec{k},\sigma}\left[\frac{\partial V_{\vec{k}}}{\partial k_\mu}c^\dagger_{\vec{k}\sigma}f_{\vec{k}\sigma}+\frac{\partial V^*_{\vec{k}}}{\partial k_\mu}f^\dagger_{\vec{k}\sigma}c_{\vec{k}\sigma}\right]+\sum_{\vec{k},\sigma}\frac{\partial\epsilon_{f\vec{k}\sigma}}{\partial k_\mu}f^\dagger_{\vec{k}\sigma}f_{\vec{k}\sigma}\ . \tag{2.3}$$

Here $\epsilon_{c\vec{k}\sigma}$ and $\epsilon_{f\vec{k}\sigma}$ are uncorrelated band energies for the s and f electrons, respectively, and $V_{\vec{k}}$ is the hybridization between s and f electrons.

B. The general formula for the electrical conductivity: the Kubo formula

The electrical conductivity tensor $\sigma_{\mu\nu}(\omega)$ under an external electric field with frequency ω is exactly given by the Kubo formula[5] in terms of the double-time Green's function[8] $Q^R_{\mu\nu}(\omega)$:

$$\sigma_{\mu\nu}(\omega)=-\frac{1}{i\omega}[Q^R_{\mu\nu}(\omega)-Q^R_{\mu\nu}(0)]\ , \tag{2.4}$$
$$Q^R_{\mu\nu}(\omega)=\int_{-\infty}^{\infty}dt\,e^{i\omega t}Q^R_{\mu\nu}(t)\ , \tag{2.5}$$
$$Q^R_{\mu\nu}(t)=\frac{1}{iV_c}\theta(t)\langle\langle[\hat{J}_\mu(t),\hat{J}_\nu(0)]\rangle\rangle\ . \tag{2.6}$$

Here V_c is the crystal volume, $\theta(t)$ is the Heaviside unit step function, and $\langle\langle\ \rangle\rangle$ is the grand canonical ensemble average with respect to the total Hamiltonian $\hat{H}$:

$$\langle\langle F\rangle\rangle=\mathrm{Tr}(e^{-\beta\hat{H}}F)/\mathrm{Tr}e^{-\beta\hat{H}}\ . \tag{2.7}$$

The current operator is written in the Heisenberg representation

$$\hat{J}_\mu(t)=e^{i\hat{H}t}J_\mu e^{-i\hat{H}t}\ . \tag{2.8}$$

The electrical resistivity tensor $R_{\mu\nu}$ is given by the inverse of the conductivity tensor

$$R_{\mu\nu}=(\sigma^{-1})_{\mu\nu}\ . \tag{2.9}$$

C. The functional integral representation of the thermodynamic Green's function

In order to calculate the double-time Green's function, we introduce the corresponding thermodynamic Green's function[8,9]

$$Q_{\mu\nu}(\tau)=-\frac{1}{V_c}\langle\langle T_\tau\hat{J}_\mu(\tau)\hat{J}_\nu(0)\rangle\rangle\ , \tag{2.10}$$
$$\hat{J}_\mu(\tau)=e^{\tau\hat{H}}\hat{J}_\mu e^{-\tau\hat{H}}\ , \tag{2.11}$$

where T_τ is the time ordering operator for fermions. We expand the thermodynamic Green's function in Fourier series with respect to τ

$$Q_{\mu\nu}(\tau)=\frac{1}{\beta}\sum_\lambda Q_{\mu\nu}(i\omega_\lambda)e^{-i\omega_\lambda\tau}\ , \tag{2.12}$$
$$\omega_\lambda=\frac{2\pi\lambda}{\beta},\quad \lambda=0,\pm1,\pm2,\ldots\ . \tag{2.13}$$

The Fourier transformation of the double-time Green's function and the Fourier coefficient of the thermodynamic Green's function are related by the analytic continuation[8,9]

$$Q^R_{\mu\nu}(\omega)=Q_{\mu\nu}(\omega+i0^+)\ . \tag{2.14}$$

Then the electrical conductivity can be calculated from the thermodynamic Green's function. In the following, we calculate the thermodynamic Green's function.

Equation (2.10) can be expressed in the functional integral representation [see Eqs. (A15)—(A19) in I]

$$Q_{\mu\nu}(\tau)=\langle Q^v_{\mu\nu}(\tau)\rangle_{\mathrm{FA}}\ , \tag{2.15}$$
$$Q^v_{\mu\nu}(\tau)=-\frac{1}{V_c}\frac{\langle T_\tau\hat{J}_\mu(\tau)\hat{J}_\nu S(\beta)\rangle}{\langle S(\beta)\rangle}\ . \tag{2.16}$$

Here subscript FA means the functional average with the distribution function of fictitious random fields, and $\langle\ \rangle$ denotes the grand canonical ensemble average with respect to the unperturbed Hamiltonian $\hat{H}_0$:

$$\langle F\rangle=\mathrm{Tr}(e^{-\beta\hat{H}_0}F)/\mathrm{Tr}e^{-\beta\hat{H}_0}\ . \tag{2.17}$$

All operators are expressed in the interaction representation. For example, the total electric current is

$$\hat{J}_\mu(\tau)=e^{\tau\hat{H}_0}J_\mu e^{-\tau\hat{H}_0}\ . \tag{2.18}$$

From the above, the procedure of calculating the electrical conductivity is summarized as follows. First, we calculate the Green's function $Q^v_{\mu\nu}(\tau)$ of particles moving in a random potential field. Second, we calculate the thermodynamic Green's function $Q_{\mu\nu}(\tau)$ by use of the functional integral of the random field. Third, we obtain the double-time Green's function through the analytic continuation, then the electrical conductivity by use of the Kubo formula. The procedure holds for the calculation of the general admittance[5] as well as the conductivity.

D. The thermodynamic Green's function in the model Hamiltonian

Before the calculation of the right-hand side of Eq. (2.16), we make assumptions on the velocity operator given by Eq. (2.3) for the sake of simplicity. The f electron in a rare-earth atom is confined within a narrow space, then the $\vec{k}$ dependence of the band energy $\epsilon_{f\vec{k}\sigma}$ is weaker than that of $\epsilon_{c\vec{k}\sigma}$. We also assume that the $\vec{k}$ dependence of the hybridization $V_{\vec{k}}$ is weak in comparison with $\epsilon_{c\vec{k}\sigma}$. Then the electric current operator is given by

$$\hat{J}_\mu=e\sum_{\vec{k},\sigma}v_\mu(\vec{k})c^\dagger_{\vec{k}\sigma}c_{\vec{k}\sigma}\ , \tag{2.19}$$

$$v_\mu(\vec{k})=\frac{\partial \epsilon_{c\vec{k}\sigma}}{\partial k_\mu} . \tag{2.20}$$

Substituting Eq. (2.19) into Eq. (2.16), we can express the thermodynamic Green's function of electrons moving in a random field in terms of the two-particle Green's function of the s electron,

$$Q^v_{\mu\nu}(\tau)=-\frac{e^2}{V_c}\sum_{\vec{k},\sigma}\sum_{\vec{k}',\sigma'} v_\mu(\vec{k})v_\nu(\vec{k})G^{\mathrm{II}v}_{c\vec{k}\sigma,c\vec{k}'\sigma';c\vec{k}\sigma,c\vec{k}'\sigma'}(\tau,0;\tau,0) , \tag{2.21}$$

$$G^{\mathrm{II}v}_{c\vec{k}\sigma,c\vec{k}'\sigma';c\vec{k}\sigma,c\vec{k}'\sigma'}(\tau,0;\tau,0)=-\frac{\langle T_\tau c_{\vec{k}\sigma}(\tau)c_{\vec{k}'\sigma'}c^\dagger_{\vec{k}\sigma}(\tau)c^\dagger_{\vec{k}'\sigma'}S(\beta)\rangle}{\langle S(\beta)\rangle} , \tag{2.22}$$

Here rearrangement is done to the time-ordering product of fermion operators.

The two-particle Green's function of the s electron moving in a random field can be factorized into the product of the one-particle Green's function as follows. We rewrite Eq. (2.22) by use of the Fourier transformation

$$G^{\mathrm{II}v}_{c\vec{k}\sigma,c\vec{k}'\sigma';c\vec{k}\sigma,c\vec{k}'\sigma'}(\tau,0;\tau,0)=\frac{1}{N^2}\sum_{i,j,l,m} e^{-i\vec{k}\cdot\vec{R}_i-i\vec{k}'\cdot\vec{R}_l+i\vec{k}\cdot\vec{R}_m+i\vec{k}'\cdot\vec{R}_j}G^{\mathrm{II}v}_{ci\sigma,cl\sigma';cm\sigma,cj\sigma'}(\tau,0;\tau,0) , \tag{2.23}$$

$$G^{\mathrm{II}v}_{ci\sigma,cl\sigma';cm\sigma,cj\sigma'}(\tau,0;\tau,0)=-\frac{\langle T_\tau c_{i\sigma}(\tau)c_{l\sigma'}c^\dagger_{m\sigma}(\tau)c^\dagger_{j\sigma'}S(\beta)\rangle}{\langle S(\beta)\rangle} . \tag{2.24}$$

In Appendix A we show that the two-particle Green's function of the electron moving in a one-body potential field can be decoupled exactly into the difference of products of two one-particle Green's functions. Applying Eq. (A2) in Appendix A to Eq. (2.24), and dropping out the τ-independent term that does not contribute to the electrical conductivity, which is easily seen from Eq. (2.4), we obtain

$$G^{\mathrm{II}v}_{ci\sigma,cl\sigma';cm\sigma,cj\sigma'}(\tau,0;\tau,0) = -G^v_{ci\sigma,cj\sigma'}(\tau,0)G^v_{cl\sigma',cm\sigma}(0,\tau) . \tag{2.25}$$

The above result, Eqs. (2.21)—(2.25), gives the expressions of the thermodynamic Green's function of the s electron moving in a random field in terms of the one-particle Green's functions of the s electron moving in a random field. In order to proceed further, we have to introduce approximations, which is the purpose of the next section.

III. APPROXIMATIONS

We calculate the two-particle Green's function and the electrical conductivity with the static approximation and the single-site CPA described in I. In the calculation of the two-particle Green's function, the static approximation decomposes the τ dependence of Eq. (2.25) into a simple form, and the single-site CPA makes it easy to take the average of Eq. (2.25) with respect to the random field. In the following we show the procedure.

A. The static approximation

In I we showed that in the static approximation

$$v_{i\sigma}(\tau)=v_{i\sigma}=\text{const} , \tag{3.1}$$

the one-particle Green's function of the electron moving in a random field depends on the difference $\tau-\tau'$:

$$G^v_{ai\sigma,bj\sigma'}(\tau,\tau')=\frac{1}{\beta}\sum_n G^v_{ai\sigma,bj\sigma'}(i\omega_n)e^{-i\omega_n(\tau-\tau')} \equiv G^v_{ai\sigma,bj\sigma'}(\tau-\tau') ,$$

$$\omega_n=\frac{2n+1}{\beta}\pi, \quad n=0,\pm1,\pm2,\ldots . \tag{3.2}$$

Then the product of the one-particle Green's function in the right-hand side of Eq. (2.25) becomes

$$G^v_{ci\sigma,cj\sigma'}(\tau,0)G^v_{cl\sigma',cm\sigma}(0,\tau)=\frac{1}{\beta}\sum_\lambda e^{-i\omega_\lambda\tau}\frac{1}{\beta}\sum_{n,n'}\delta_{\lambda,n-n'}G^v_{ci\sigma,cj\sigma'}(i\omega_n)G^v_{cl\sigma',cm\sigma}(i\omega_{n'}) . \tag{3.3}$$

Then we obtain from Eqs. (2.15), (2.21), (2.23), (2.25), and (3.3)

$$Q_{\mu\nu}(\tau)=\frac{1}{\beta}\sum_\lambda e^{-i\omega_\lambda\tau}Q_{\mu\nu}(i\omega_\lambda) , \tag{3.4}$$

$$Q_{\mu\nu}(i\omega_\lambda)=\frac{e^2}{V_c}\sum_{\vec{k},\sigma}\sum_{\vec{k}',\sigma'} v_\mu(\vec{k})v_\nu(\vec{k}')\frac{1}{\beta}\sum_{n,n'}\delta_{\lambda,n-n'}G^{\mathrm{II}}_{c\vec{k}\sigma,c\vec{k}'\sigma';c\vec{k}'\sigma',c\vec{k}\sigma}(i\omega_n,i\omega_{n'}) , \tag{3.5}$$

$$G^{\mathrm{II}}_{c\vec{k}\sigma,c\vec{k}'\sigma';c\vec{k}'\sigma',c\vec{k}\sigma}(i\omega_n,i\omega_{n'})=\frac{1}{N^2}\sum_{i,j,l,m} e^{-i\vec{k}\cdot\vec{R}_i-i\vec{k}'\cdot\vec{R}_l+i\vec{k}\cdot\vec{R}_m+i\vec{k}'\cdot\vec{R}_j}\langle G^v_{ci\sigma,cj\sigma'}(i\omega_n)G^v_{cl\sigma',cm\sigma}(i\omega_{n'})\rangle_{FA} . \tag{3.6}$$

In the next section we calculate the right-hand side of Eq. (3.6) according to the single-site CPA.

B. The single-site CPA

In the static approximation and the single-site CPA, the functional integral becomes a simple product of the integrals with respect to the single-site variables as described in I. We show in Appendix B the procedure for calculating the average of the product of the one-particle Green's function of an electron moving in a random potential field within the single-site CPA. Substituting Eqs. (B8) and (B9) into Eq. (3.6), we obtain

$$G^{\mathrm{II}}_{c\vec{k}\sigma,c\vec{k}'\sigma';c\vec{k}'\sigma',c\vec{k}\sigma}(i\omega_n,i\omega_{n'})=\delta_{\sigma\sigma'}\left[G^{\sigma}_{cc}(\vec{k},i\omega_n)G^{\sigma}_{cc}(\vec{k}',i\omega_{n'})\right.$$
$$\left.+G^{\sigma}_{fc}(\vec{k},i\omega_n)G^{\sigma}_{cf}(\vec{k},i\omega_{n'})\frac{1}{N}\Gamma(i\omega_n,i\omega_{n'})G^{\sigma}_{fc}(\vec{k}',i\omega_{n'})G^{\sigma}_{cf}(\vec{k}',i\omega_n)\right], \tag{3.7}$$

$$\Gamma(i\omega_n,i\omega_{n'})=\frac{\gamma(i\omega_n,i\omega_{n'})}{1-\gamma(i\omega_n,i\omega_{n'})\Xi(i\omega_n,i\omega_{n'})}, \tag{3.8}$$

$$\Xi(i\omega_n,i\omega_{n'})=\frac{1}{N}\sum_{\vec{p}}G^{\sigma}_{ff}(\vec{p},i\omega_n)G^{\sigma}_{ff}(\vec{p},i\omega_{n'}). \tag{3.9}$$

Here the function Γ depends only on $i\omega_n$ and $i\omega_{n'}$. The $\vec{k}$ independence of Γ arises from the $\vec{k}$ independence of Ξ, which is a result of the single-site CPA. The second term of the right-hand side in Eq. (3.7) is the so-called vertex correction.

C. The thermodynamic and double-time Green's functions

Substituting Eq. (3.7) into Eq. (3.5), we obtain

$$Q_{\mu\nu}(i\omega_\lambda)=\frac{e^2}{V_c}\sum_{\sigma}\frac{1}{\beta}\sum_{n,n'}\delta_{\lambda,n-n'}\left[\sum_{\vec{k}}v_\mu(\vec{k})v_\nu(\vec{k})G^{\sigma}_{cc}(\vec{k},i\omega_n)G^{\sigma}_{cc}(\vec{k},i\omega_{n'})\right.$$
$$+\sum_{\vec{k}}v_\mu(\vec{k})G^{\sigma}_{fc}(\vec{k},i\omega_n)G^{\sigma}_{cf}(\vec{k},i\omega_{n'})\frac{1}{N}\Gamma(i\omega_n,i\omega_{n'})$$
$$\left.\times\sum_{\vec{k}'}v_\nu(\vec{k}')G^{\sigma}_{fc}(\vec{k}',i\omega_{n'})G^{\sigma}_{cf}(\vec{k}',i\omega_n)\right]. \tag{3.10}$$

By virtue of the time-reversal symmetry

$$\epsilon(\vec{k})=\epsilon(-\vec{k}),\quad v_\mu(\vec{k})=-v_\mu(-\vec{k}), \tag{3.11}$$

the one-particle Green's function is an even function of $\vec{k}$, then the second term in the large parentheses of Eq. (3.10) identically vanishes after $\vec{k}$ summation. Then the thermodynamic Green's function reduces to

$$Q_{\mu\nu}(i\omega_\lambda)=\frac{e^2}{V_c}\sum_{\sigma}\sum_{\vec{k}}v_\mu(\vec{k})v_\nu(\vec{k})\frac{1}{\beta}\sum_{n}G^{\sigma}_{cc}(\vec{k},i\omega_n+i\omega_\lambda)G^{\sigma}_{cc}(\vec{k},i\omega_n). \tag{3.12}$$

Transforming the summation with respect to n into a contour integral in the complex plane, and performing the analytic continuation $i\omega_\lambda\rightarrow\omega+i0^+$, we obtain the double-time Green's function

$$Q^{R}_{\mu\nu}(\omega)=Q_{\mu\nu}(\omega+i0^+)$$
$$=\frac{e^2}{\pi V_c}\sum_{\sigma}\sum_{\vec{k}}v_\mu(\vec{k})v_\nu(\vec{k})\int_{-\infty}^{\infty}dz\{-f(z)G^{\sigma}_{cc}(\vec{k},z+\omega+i0^+)\mathrm{Im}[G^{\sigma}_{cc}(\vec{k},z+i0^+)]$$
$$-f(z+\omega)\mathrm{Im}[G^{\sigma}_{cc}(\vec{k},z+\omega+i0^+)]G^{\sigma}_{cc}(\vec{k},z-i0^+)\}, \tag{3.13}$$

where Im means the imaginary part and $f(z)$ is the Fermi-Dirac distribution function

$$f(z)=(e^{\beta z}+1)^{-1}. \tag{3.14}$$

D. The electrical conductivity

In the formula of the electrical conductivity given by Eq. (2.4), it is the real part that contributes to the energy absorption. From Eq. (3.13) we obtain

$$\mathrm{Re}\sigma_{\mu\nu}(\omega)=-\frac{1}{\omega}\mathrm{Im}Q^{R}_{\mu\nu}(\omega)$$
$$=\frac{e^2}{\pi V_c}\sum_{\vec{k},\sigma} v_\mu(\vec{k})v_\nu(\vec{k})\int_{-\infty}^{\infty}dz\frac{1}{\omega}[f(z)-f(z+\omega)]\mathrm{Im}[G^{\sigma}_{cc}(\vec{k},z+\omega+i0^+)]\mathrm{Im}[G^{\sigma}_{cc}(\vec{k},z+i0^+)]\ . \tag{3.15}$$

This is the general formula for the electrical conductivity of the s electron in the periodic Anderson model under the static approximation and the single-site CPA. Especially, in the limit of ω tending to zero, we obtain the static conductivity

$$\mathrm{Re}\sigma_{\mu\nu}(0)=\frac{e^2}{\pi V_c}\sum_{\vec{k},\sigma} v_\mu(\vec{k})v_\nu(\vec{k})\int_{-\infty}^{\infty}dz\left[-\frac{\partial f}{\partial z}\right]\{\mathrm{Im}[G^{\sigma}_{cc}(\vec{k},z+i0^+)]\}^2\ , \tag{3.16}$$

which is the same form as Velicky's formula[10] for random alloys.

IV. A MODEL BAND

A. Model band parameters

In order to carry out the $\vec{k}$ summation in Eqs. (3.15) and (3.16), we have to set the model band parameters $\epsilon_{c\vec{k}\sigma}$, $\epsilon_{f\vec{k}\sigma}$, and $V_{\vec{k}}$. As described in I, we neglect the $\vec{k}$ dependence of $\epsilon_{f\vec{k}\sigma}$ and $V_{\vec{k}}$, which is suitable for rare-earth compounds:

$$\epsilon_{f\vec{k}\sigma}=\epsilon_{f\sigma}\ \text{ for all } \vec{k} \tag{4.1}$$

$$V_{\vec{k}}=V\ \text{ for all } \vec{k}\ . \tag{4.2}$$

Under these assumptions, the $\vec{k}$ dependence of the one-particle Green's function arises from $\epsilon_{c\vec{k}\sigma}$. The uncorrelated density of states $\rho^0_\sigma(\epsilon)$ of the s electron is

$$\rho^0_\sigma(\epsilon)=\frac{1}{N}\sum_{\vec{k}}\delta(\epsilon-\epsilon_{c\vec{k}\sigma})\ . \tag{4.3}$$

We introduce a function $A^{\sigma}_{\mu\nu}(\epsilon)$ given by

$$A^{\sigma}_{\mu\nu}(\epsilon)=\frac{1}{N}\sum_{\vec{k}} v_\mu(\vec{k})v_\nu(\vec{k})\delta(\epsilon-\epsilon_{c\vec{k}\sigma})\ . \tag{4.4}$$

Then Eq. (3.15) becomes

$$\mathrm{Re}\sigma_{\mu\nu}(\omega)=\frac{e^2}{\pi\bar{\Omega}}\sum_{\sigma}\int_{-\infty}^{\infty}dz\frac{1}{\omega}[f(z)-f(z+\omega)]\int_{-\infty}^{\infty}d\epsilon A^{\sigma}_{\mu\nu}(\epsilon)\mathrm{Im}[G^{\sigma}_{cc}(\epsilon,z+\omega+i0^+)]\mathrm{Im}[G^{\sigma}_{cc}(\epsilon,z+i0^+)]\ . \tag{4.5}$$

Here $\bar{\Omega}$ is a volume per site $\bar{\Omega}=V_c/N$, and the one-particle Green's function of the s electron is[1]

$$G^{\sigma}_{cc}(\epsilon,z)=[F_\sigma(z)-\tilde{\epsilon}\,]^{-1}\ ,$$
$$F_\sigma(z)=z-|V|^2/[z-\tilde{\epsilon}_{f\sigma}-\Sigma_\sigma(z)]\ , \tag{4.6}$$

where $\tilde{\epsilon}=\epsilon-\mu$, $\tilde{\epsilon}_{f\sigma}=\epsilon_{f\sigma}-\mu$, and μ is the chemical potential.

The conductivity at 0 K shows characteristic properties of the interband transition specified by the solution z_i of the equation (the condition of zero-momentum transfer)

$$F_\sigma(z+\omega)-F_\sigma(z)=0\ .$$

The lower and upper bounds of ω that the conductivity is nonzero at 0 K are determined as follows. The lower bound ω_{LB} is given by the minimum of the band gap between hybridized subbands in energy-momentum space: $\omega_{\mathrm{LB}}=2|V|$. The conductivity at 0 K is zero for $\omega<\omega_{\mathrm{LB}}$ and contains a factor $(\omega^2-4|V|^2)^{-1/2}$ for $\omega>\omega_{\mathrm{LB}}$. The singularity at ω_{LB} comes from the simultaneous condition of zero-momentum transfer and the equality of group velocity $[F'_\sigma(z+\omega)-F'_\sigma(z)=0]$. This is the so-called Van Hove singularity. The upper bound ω_{UB} is determined by the condition that the one real solution z_i at least should lie within the interval between $-\omega$ and 0, and the value $F_\sigma(z_i)+\mu$ should lie within the uncorrelated s-electron band. The upper bound depends on the model band parameters.

B. A model density of states

We assume the elliptic model density of states introduced in I

$$\rho^0_\sigma(\epsilon)=\begin{cases}(2/\pi)(1-\epsilon^2)^{1/2}, & -1\le\epsilon\le 1\\ 0, & \text{otherwise}\end{cases} \tag{4.7}$$

where the half band width is taken to be unity. In addition, we assume the following form of the diagonal element of $A^{\sigma}_{\mu\nu}(\epsilon)$:

$$A^{\sigma}_{\mu\mu}(\epsilon)=\frac{8\pi}{3\alpha}(1-\epsilon^2)^{3/2}\ , \tag{4.8}$$

which reproduces the correct expansion near the band edges $\epsilon_{c\vec{k}\sigma}\simeq\pm\alpha k^2\mp 1$.

Substituting Eq. (4.8) into Eq. (4.5), we obtain the diagonal element of the real part of the dynamical conductivity

$$\mathrm{Re}\sigma(\omega)=\frac{2e^2}{\pi\bar{\Omega}}\int_{-\infty}^{\infty}dz\frac{1}{\omega}[f(z)-f(z+\omega)]H(z,\omega)\ . \tag{4.9}$$

Here a factor 2 arises from the summation with respect to the spin variable in the paramagnetic state, and the function $H(z,\omega)$ that contains a factor $\mathrm{Im}[G_{cc}(z+\omega)]\times\mathrm{Im}[G_{cc}(z)]$ is given by

$$H(z,\omega)=\frac{\alpha}{3}\left[\mathrm{Im}[G_{cc}(z)]\mathrm{Im}[G_{cc}(z+\omega)]-2\mathrm{Re}\left[\frac{[G_{cc}(z)-G_{cc}(z+\omega)]^2}{G_{cc}(z)G_{cc}(z+\omega)-4}-\frac{[\bar{G}_{cc}(z)-G_{cc}(z+\omega)]^2}{\bar{G}_{cc}(z)G_{cc}(z+\omega)-4}\right]\right], \tag{4.10}$$

$$G_{cc}(z)=2(F(z)-\{[F(z)]^2-1\}^{1/2}), \tag{4.11}$$

where $G_{cc}(z)$ is the diagonal element of the one-particle Green's function in the site representation.[1] The diagonal element of the static conductivity is also given by

$$\mathrm{Re}\sigma(0)=\frac{2e^2}{\pi\Omega}\int_{-\infty}^{\infty}dz\left[-\frac{\partial f}{\partial z}\right]H(z), \tag{4.12}$$

$$H(z)=\frac{\alpha}{3}\{\mathrm{Im}[G_{cc}(z)]\}^2\left[1-\frac{8}{G_{cc}(z)\bar{G}_{cc}(z)-4}\right]. \tag{4.13}$$

V. NUMERICAL CALCULATION

We make assumptions on the parameters as described in I. The electron number per site is assumed to be two including the spin degeneracy

$$N_e/N=2. \tag{5.1}$$

In this case the electronic state is insulating at 0 K. For the sake of simplicity, we assume the electron-hole symmetry

$$\epsilon_{f\sigma}=-U/2. \tag{5.2}$$

In this case the chemical potential does not depend on temperature, so we take the origin of the energy to the chemical potential

$$\mu=0. \tag{5.3}$$

Under these assumptions we show the numerical results for the hybridization $V=0.3$ and the Coulomb repulsion $U=0.6$ in units of the halfwidth of the uncorrelated s electron band. The combination of these two parameters is a typical case. The paramagnetic state near the boundary of the formation of the local moment is realized at 0 K. And the hybridization gap vanishes at sufficiently low temperature in comparison with the width of the uncorrelated s-electron band.

A. Temperature dependence of the electrical resistivity

We show the temperature dependence of the electrical resistivity in Fig. 1. We depict the transition temperature T_c by an arrow where the hybridization gap vanishes. The transition temperature is 0.0255 in units of the halfwidth of the uncorrelated s-electron band. The temperature dependence of the electrical resistivity is quite different below and above T_c.

Below T_c the electron system is a paramagnetic semiconductor. At 0 K, the electrical resistivity is infinite because the conductivity is zero, which is easily seen from Eq. (3.16). With increasing temperature, the electrical resistivity lowers with an order of magnitude. The electrical resistivity decreases more slowly than that of the usual intrinsic semiconductors[11] with the constant energy gap. It can be interpreted as follows: The spin-field fluctuation makes the hybridization gap decrease and accelerates thermal excitation of electrons. At the same time, however, the spin-field fluctuation scatters the s electron because it breaks translational invariance of the electron system. The effect of the s-electron scattering due to the spin-field fluctuation partially cancels the decrease of the electrical resistivity due to thermal excitation of electrons.

Above T_c the temperature dependence of the electrical resistivity is relatively weak in comparison with that below T_c. The electrical resistivity decreases rapidly at the initial stage then slowly with increasing temperature above T_c. This rapid and slow decrease of the electrical resistivity corresponds to the rapid and slow increase of the density of states of the s electron at the chemical potential.[1] The electrical resistivity continuously decreases below and above T_c because of the temperature dependence of the Fermi-Dirac distribution function.

In Fig. 1 we also show the plot of the electrical resistivity versus inverse temperature. We can easily see that the graph is lower convex below T_c and upper convex above T_c. Even below T_c linearity of the logarithm of the electrical resistivity versus inverse temperature, which is seen in the usual intrinsic semiconductors, does not hold.

B. Temperature dependence of the dynamical conductivity

The electrical resistivity is the inverse of the electrical conductivity at the zero frequency. We can get a clearer insight into the nonmetal-metal transition with the study of the dynamical conductivity. Because the real part of the dynamical conductivity (RPDC) directly relates to the

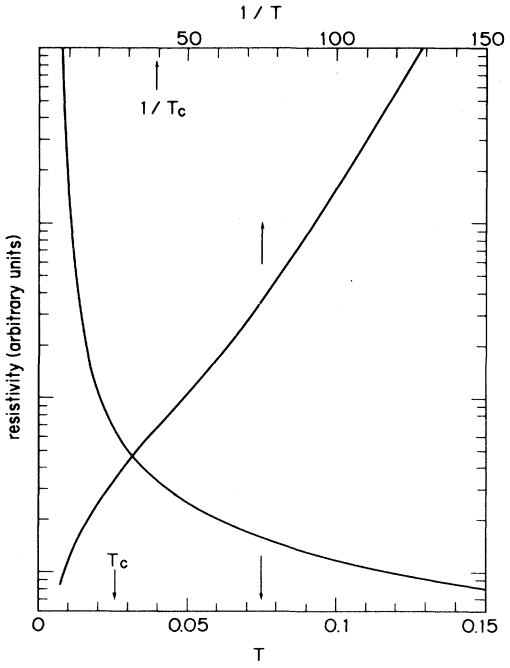

FIG. 1. Temperature dependence of the electrical resistivity. Temperature is measured in units of the halfwidth of the uncorrelated s-electron band.

energy absorption of the electron system.

We show the temperature dependence of the RPDC in Fig. 2. The density of states is shown in Fig. 4 ($\langle\xi^2\rangle=0.01$—0.1) in I. We first explain the RPDC below T_c. At 0 K, the RPDC is nonzero between the frequencies $\omega_{\rm LB}=2\,|\,V\,|$ and $\omega_{\rm UB}=(1+4\,|\,V\,|^2)^{1/2}$. The RPDC has a Van Hove—type singularity at $\omega_{\rm LB}$. At very low temperature ($T=0.00786$), the RPDC still has a "semiconducting" profile. The RPDC is small at the zero frequency. It grows rapidly at the corresponding frequency of the hybridization gap. The sharp maximum of the RPDC near $\omega=2\,|\,V\,|$ comes from the singular peak at 0 K. At high frequency, the RPDC declines with the Drude tail and vanishes at the frequency equal to the energy difference between the top of the upper band and the bottom of the lower band. With increasing temperature ($T=0.0157$, 0.0236), the profile of the RPDC changes drastically. The most salient feature is that the maximum of the RPDC near the frequency $\omega=2\,|\,V\,|$ decreases rapidly and that the RPDC near the zero frequency grows gradually, because growth of the imaginary part of the self-energy with increasing temperature yields the spread of the bands, i.e., the decrease of the hybridization gap. The Drude tail at high frequency, however, does not change appreciably because the density of states near the top of the upper band and the bottom of the lower band does not depend on temperature strongly compared with that of the hybridization gap. The RPDC at the zero frequency is finite even below T_c. It arises from the temperature dependence of the Fermi-Dirac distribution function. This corresponds to the rapid decrease of the electrical resistivity below T_c in Fig. 1 with increasing temperature. We notice that if we approximate the Fermi-Dirac distribution function to the step function, then the RPDC has a sharp absorption edge and the RPDC at the zero frequency remains zero below T_c.

Next we refer to the RPDC above T_c. With increasing temperature, the RPDC near the zero frequency grows. The frequency where the RPDC is a maximum remains nonzero even above T_c ($T=0.0314$—0.0550), then shifts to zero with further increasing temperature ($T=0.0629$—0.0782). The RPDC at high temperature has a maximum at the zero frequency, and decreases with a Drude tail. This overall behavior corresponds to the intraband energy absorption of metals.

In conclusion, we note that the profile of the RPDC changes from a semiconducting one well below T_c to a metallic one well above T_c. The change is smooth and continuous with increasing temperature.

C. Comparison with experiment

We compare our result with experiment. We first discuss the temperature dependence of the electrical resistivity. Experimental results of the electrical resistivity in SmB_6 are as follows.[12–17] The electrical resistivity at room temperature is about 500 $\mu\Omega$ cm, and SmB_6 is a poor metal. With decreasing temperature, the resistivity increases appreciably. With further decreasing temperature (about 50—6 K), the resistivity increases gradually at first and then rapidly 4 orders of magnitude. Below 6 K, the resistivity saturates and does not depend on temperature. These results are compared with our result. We first compare our result with experiment above 6 K. Our result qualitatively agrees well with experimental result. Namely, in our theory, with decreasing temperature ($T=0.1\sim T_c$), the resistivity increases slowly at first, then increases at slightly above T_c, and at last abruptly with orders of magnitude below T_c. Second, the saturation of the resistivity at very low temperature can be naturally understood if we consider the effect of impurities contained within samples.[11] Third, the Arrhenius plot of the electrical resistivity versus inverse temperature is not a straight line below T_c. Such a tendency has been seen in the experimental results.[17] Our theory also can be applied to the nonmetal-metal transition in SmS under pressure.[18]

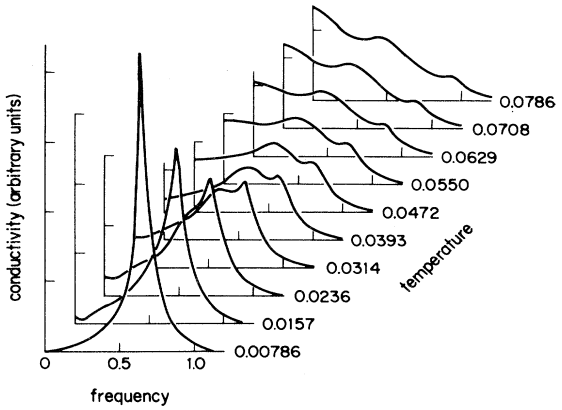

FIG. 2. Temperature dependence of the real part of the dynamical conductivity. Frequency and temperature are measured in units of the halfwidth of the uncorrelated s-electron band.

We next discuss the temperature dependence of the dynamical conductivity. Recent experiments[2,16] show that the RPDC at 4 K has a deep minimum at the zero frequency and the RPDC at room temperature has no dip at the zero frequency. These experimental results qualitatively agree well with our results.

ACKNOWLEDGMENTS

The author wishes to thank Professor M. Inoue, Professor Y. Onodera, and Dr. K. Fukushima.

APPENDIX A: THE TWO-PARTICLE GREEN'S FUNCTION OF AN ELECTRON MOVING IN A ONE-BODY POTENTIAL FIELD

The two-particle Green's function of an electron moving in a one-body potential field is defined by

$$G^{\rm II\,v}_{\alpha i,\beta l;\gamma m,\delta j}(\tau_1,\tau_2;\tau_3,\tau_4)=-\frac{\langle T_\tau \alpha_i(\tau_1)\beta_l(\tau_2)\gamma^\dagger_m(\tau_3)\delta^\dagger_j(\tau_4)S(\beta)\rangle}{\langle S(\beta)\rangle}\,, \tag{A1}$$

where the operators α, β, γ, and δ denote c or f, and the subscripts i, j, l, and m denote both the site and spin variables. Substituting the series expansion of $S(\beta)$ given by Eq. (A13) in I into (A1), and using the Bloch—de Dominicis theorem with the diagram technique, we can exactly express the right-hand side of (A1) into the difference of the products of the one-particle Green's functions of an electron moving in a one-body potential field:

$$G^{\mathrm{II}\,v}_{\alpha i,\beta l;\gamma m,\delta j}(\tau_1,\tau_2;\tau_3,\tau_4)=G^{v}_{\alpha i,\gamma m}(\tau_1,\tau_3)G^{v}_{\beta l,\delta j}(\tau_2,\tau_4)-G^{v}_{\alpha i,\delta j}(\tau_1,\tau_4)G^{v}_{\beta l,\gamma m}(\tau_2,\tau_3)\ , \tag{A2}$$

where $G^{v}_{\alpha i,\beta j}(\tau,\tau')$ is the exact one-particle Green's function of an electron moving in a one-body potential field.[1] We show the diagrams of the two-particle Green's functions of the f and s electrons in Fig. 3.

APPENDIX B: THE AVERAGE OF THE PRODUCT OF THE ONE-PARTICLE GREEN'S FUNCTIONS WITH RESPECT TO THE RANDOM-FIELD VARIABLES

We calculate the average of the product of the one-particle Green's functions with respect to the random-field variables in the single-site CPA:

$$\langle [G^{v}_{\alpha\beta}(z_1)]_{ij}[G^{v}_{\gamma\delta}(z_2)]_{lm}\rangle_{FA}\ , \tag{B1}$$

where the operators α, β, γ, and δ denote c or f, and the subscripts i, j, l, and m denote the site and spin variables. We also derive Ward's relations. In order to simplify the notation, we denote the average $\langle\ \rangle_{FA}$ to the simple notation $\langle\ \rangle$ in the following.

From the series expansion of the one-particle Green's function given by Eq. (4.3) in I, we obtain

$$\begin{aligned}&\langle [G^{v}_{\alpha\beta}(z_1)]_{ij}[G^{v}_{\gamma\delta}(z_2)]_{lm}\rangle\\&=\Big\langle \Big[[g_{\alpha\beta}(z_1)]_{ij}+\sum_a [g_{\alpha f}(z_1)]_{ia}v_a[g_{f\beta}(z_1)]_{aj}+\sum_{a,b}[g_{\alpha f}(z_1)]_{ia}v_a[g_{ff}(z_1)]_{ab}v_b[g_{f\beta}(z_1)]_{bj}+\cdots\Big]\\&\quad\times\Big[[g_{\gamma\delta}(z_2)]_{lm}+\sum_s [g_{\gamma f}(z_2)]_{ls}v_s[g_{f\delta}(z_2)]_{sm}+\sum_{s,t}[g_{\gamma f}(z_2)]_{ls}v_s[g_{ff}(z_2)]_{st}v_t[g_{f\delta}(z_2)]_{tm}+\cdots\Big]\Big\rangle\ .\end{aligned} \tag{B2}$$

We expand the right-hand side of Eq. (B2) term by term, and replace the average of the powers of the random-field variables by the cummulant average.[19] In order to maintain the internal consistency within the single-site CPA, we drop the terms that connect over two sites or more in the one-particle Green's function and the vertex part. Such terms appear greater than or equal to fourth order in v. Introducing the proper self-energy $\Sigma(z)$ of the f electron, and taking the partial summations, we can recollect the one-particle Green's function:

$$\begin{aligned}[G_{\alpha\beta}(z)]_{ij}&\equiv\langle [G^{v}_{\alpha\beta}(z)]_{ij}\rangle\\&=[g_{\alpha\beta}(z)]_{ij}+\sum_a [g_{\alpha f}(z)]_{ia}\Sigma(z)[g_{f\beta}(z)]_{aj}+\sum_{a,b}[g_{\alpha f}(z)]_{ia}\Sigma(z)[g_{ff}(z)]_{ab}\Sigma(z)[g_{f\beta}(z)]_{bj}+\cdots\ ,\end{aligned} \tag{B3}$$

$$\begin{aligned}\Sigma(z)&=\langle v\rangle_c+\langle v^2\rangle_c[G_{ff}(z)]_{aa}+\langle v^3\rangle_c\{[G_{ff}(z)]_{aa}\}^2+\cdots\\&=\langle v\{1-v[G_{ff}(z)]_{aa}\}^{-1}\rangle_c\ ,\end{aligned} \tag{B4}$$

where $\langle\ \rangle_c$ denotes the cumulant average. By use of these expressions, we obtain from Eq. (B2)

$$\begin{aligned}&\langle [G^{v}_{\alpha\beta}(z_1)]_{ij}[G^{v}_{\gamma\delta}(z_2)]_{lm}\rangle\\&=[G_{\alpha\beta}(z_1)]_{ij}[G_{\gamma\delta}(z_2)]_{lm}+\sum_a [G_{f\alpha}(z_1)]_{ia}[G_{\delta f}(z_2)]_{am}\gamma(z_1,z_2)[G_{f\gamma}(z_2)]_{la}[G_{\beta f}(z_1)]_{aj}\\&\quad+\sum_{a,b}[G_{f\alpha}(z_1)]_{ia}[G_{\delta f}(z_2)]_{am}\gamma(z_1,z_2)[G_{ff}(z_1)]_{ab}[G_{ff}(z_2)]_{ba}\gamma(z_1,z_2)[G_{f\gamma}(z_2)]_{lb}[G_{\beta f}(z_1)]_{bj}+\cdots\ .\end{aligned} \tag{B5}$$

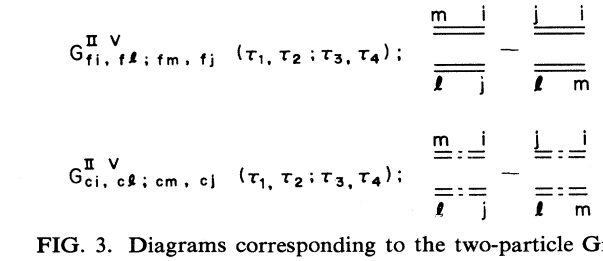

FIG. 3. Diagrams corresponding to the two-particle Green's function of f and s electrons moving in a one-body potential field.

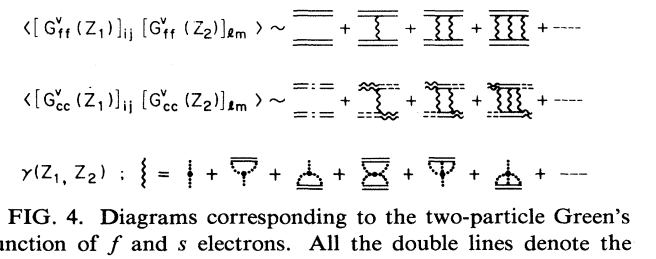

FIG. 4. Diagrams corresponding to the two-particle Green's function of f and s electrons. All the double lines denote the averaged Green's functions with respect to the random-field variables.

Here we introduce an effective interaction vertex function $\gamma(z_1,z_2)$:

$$\begin{aligned}\gamma(z_1,z_2)=&\langle v^2\rangle_c+\langle v^3\rangle_c[G_{ff}(z_1)]_{aa}+\langle v^3\rangle_c[G_{ff}(z_2)]_{aa}\\&+\langle v^4\rangle_c[G_{ff}(z_1)]_{aa}[G_{ff}(z_2)]_{aa}+\langle v^4\rangle_c\{[G_{ff}(z_1)]_{aa}\}^2+\langle v^4\rangle_c\{[G_{ff}(z_2)]_{aa}\}^2+\cdots\\=&\langle v\{1-v[G_{ff}(z_1)]_{aa}\}^{-1}v\{1-v[G_{ff}(z_2)]_{aa}\}^{-1}\rangle_c\ .\end{aligned}\tag{B6}$$

Diagrams for the f and s electrons are depicted in Fig. 4. By use of the Fourier transformation with respect to the site variable

$$[G_{\alpha\beta}(z)]_{ij}=\frac{1}{N}\sum_{\vec{k},\vec{k}'}e^{i\vec{k}\cdot\vec{R}_i-i\vec{k}'\cdot\vec{R}_j}G_{\alpha\beta}(\vec{k},z)\delta_{\vec{k},\vec{k}'}\ ,\tag{B7}$$

we obtain

$$\langle[G^v_{\alpha\beta}(z_1)]_{ij}[G^v_{\gamma\delta}(z_2)]_{lm}\rangle=\frac{1}{N^2}\sum_{\vec{k}_1,\vec{k}_2,\vec{k}_3,\vec{k}_4}e^{i\vec{k}_1\cdot\vec{R}_i-i\vec{k}_2\cdot\vec{R}_m-i\vec{k}_3\cdot\vec{R}_j+i\vec{k}_4\cdot\vec{R}_l}K(\vec{k}_1,\vec{k}_2;\vec{k}_3,\vec{k}_4;z_1,z_2)\ ,\tag{B8}$$

$$\begin{aligned}&K(\vec{k}_1,\vec{k}_2;\vec{k}_3,\vec{k}_4;z_1,z_2)\\&=G_{\alpha\beta}(\vec{k}_1,z_1)G_{\gamma\delta}(\vec{k}_2,z_2)\delta_{\vec{k}_1,\vec{k}_3}\delta_{\vec{k}_2,\vec{k}_4}+\gamma(z_1,z_2)\frac{1}{N}\delta(-\vec{k}_1+\vec{k}_2+\vec{k}_3-\vec{k}_4)G_{f\alpha}(\vec{k}_1,z_1)G_{\delta f}(\vec{k}_2,z_2)G_{f\gamma}(\vec{k}_4,z_2)G_{\beta f}(\vec{k}_3,z_1)\\&\quad+\sum_{\vec{k}_5,\vec{k}_6}\gamma(z_1,z_2)\frac{1}{N}\delta(-\vec{k}_1+\vec{k}_2+\vec{k}_5-\vec{k}_6)\gamma(z_1,z_2)\frac{1}{N}\delta(-\vec{k}_5+\vec{k}_6-\vec{k}_4+\vec{k}_3)\\&\qquad\times G_{f\alpha}(\vec{k}_1,z_1)G_{\delta f}(\vec{k}_2,z_2)G_{ff}(\vec{k}_5,z_1)G_{ff}(\vec{k}_6,z_2)G_{f\gamma}(\vec{k}_4,z_2)G_{\beta f}(\vec{k}_3,z_1)+\cdots\ .\end{aligned}\tag{B9}$$

Here we notice that the Green's function in Eqs. (B7)—(B9) should be regarded as a matrix with respect to spin variables.

We notice the relation between the self-energy given by Eq. (B4) and the effective interaction vertex function given by Eq. (B6). These two quantities are not independent, but satisfy the identities called Ward's relations. For example, we obtain

$$\gamma(z_1,z_2)=\frac{\Sigma(z_1)-\Sigma(z_2)}{[G_{ff}(z_1)]_{aa}-[G_{ff}(z_2)]_{aa}}\ ,\tag{B10}$$

$$\frac{\partial\Sigma(z)}{\partial[G_{ff}(z)]_{aa}}=\gamma(z,z)\ .\tag{B11}$$

These relations indicate the internal consistency of the single-site CPA in the vertex corrections.[10,19]

---

*Present address: Fujitsu Limited, 1015 Kamiodanaka, Nakahara-ku, Kawasaki 211, Japan.

[1]H. Ishikawa, preceding paper, Phys. Rev. B 28, 5643 (1983). This paper is referred to as I.

[2]J. W. Allen, R. M. Martin, B. Batlogg, and P. Watcher, J. Appl. Phys. 49, 2078 (1978).

[3]O. Sakai, S. Seki, and M. Tachiki, J. Phys. Soc. Jpn. 45, 1465 (1978).

[4]I. Aveline and J. R. Iglesias-Sicardi, Solid State Commun. 37, 749 (1981).

[5]R. Kubo, J. Phys. Soc. Jpn. 12, 570 (1957).

[6]H. J. Leder and B. Muhlchlegel, Z. Phys. B 29, 341 (1978).

[7]P. W. Anderson, Phys. Rev. 124, 41 (1961).

[8]R. Abe, *Statistical Physics,* (University of Tokyo Press, Tokyo, 1966) (in Japanese).

[9]A. A. Abrikosov, L. P. Gorkov, and I. E. Dzyaloshinski, *Methods of Quantum Field Theory in Statistical Physics* (Dover, New York, 1963).

[10]B. Velicky, Phys. Rev. 184, 614 (1969).

[11]C. Kittel, *Introduction to Solid State Physics,* 3rd ed. (Wiley, New York, 1966), Chap. 10.

[12]A Menth, E. Bucher, and T. H. Geballe, Phys. Rev. Lett. 22, 275 (1969).

[13]J. C. Nickerson, R. M. White, K. N. Lee, R. Bachmann, T. H. Geballe, and G. W. Hull, Jr., Phys. Rev. B 3, 2030 (1971).

[14]T. Kasuya, K. Kojima, and M. Kasaya, in *Valence Instabilities and Related Narrow Band Phenomena,* edited by R. D. Parks (Plenum, New York, 1977), p. 137.

[15]J. W. Allen, B. Batlogg, and P. Watcher, Phys. Rev. B 20, 4807 (1979).

[16]B. Batlogg, P. H. Schmit, and J. M. Rowell, in *Valence Fluctuations in Solids,* edited by L. M. Falikov, W. Hanke, and M. B. Maple (North-Holland, Amsterdam, 1981), p. 267.

[17]M. Kasaya, H. Kimura, T. Fujita, and T. Kasuya, in *Valence Fluctuations in Solids,* edited by L. M. Falikov, W. Hanke, and M. B. Maple (North-Holland, Amsterdam, 1981), p. 251.

[18]S. D. Bader, N. E. Phillips, and D. B. McWhan, Phys. Rev. B 7, 4686 (1973).

[19]F. Yonezawa and K. Morigaki, Suppl. Prog. Theor. Phys. 53, 1 (1973).